Ecological Informatics 62 (2021) 101268

Contents lists available at ScienceDirect

Ecological Informatics

journal homepage: www.elsevier.com/locate/ecolinf

The Peruvian Amazon forestry dataset: A leaf image classification corpus

Gerson Vizcarra [a], Danitza Bermejo [a,b], Antoni Mauricio [a], Ricardo Zarate Gomez [a], Erwin Dianderas [a,*]

[a] GESCON, Instituto de Investigaciones de la Amazonía Peruana (IIAP), Av. A. Quiñones km 2,5, Iquitos, Loreto 16007, Peru
[b] Universidad Nacional del Altiplano, Puno, Peru

ARTICLE INFO

Keywords:
Leaves dataset
Peruvian Amazon
Deep learning
Visual interpretation
Interpretation

ABSTRACT

Forest census allows getting precise data for logging planning and elaboration of the forest management plan. Species identification blunders carry inadequate forest management plans and high risks inside forest concessions. Hence, an identification protocol prevents the exploitation of non-commercial or endangered timber species. The current Peruvian legislation allows the incorporation of non-technical experts, called "materos", during the identification. Materos use common names given by the folklore and traditions of their communities instead of formal ones, which generally lead to misclassifications. In the real world, logging companies hire materos instead of botanists due to cost/time limitations. Given such a motivation, we explore an end-to-end software solution to automatize the species identification. This paper introduces the Peruvian Amazon Forestry Dataset, which includes 59,441 leaves samples from ten of the most profitable and endangered timber-tree species. The proposal contemplates a background removal algorithm to feed a pre-trained CNN by the ImageNet dataset. We evaluate the quantitative (accuracy metric) and qualitative (visual interpretation) impacts of each stage by ablation experiments. The results show a 96.64% training accuracy and 96.52% testing accuracy on the VGG-19 model. Furthermore, the visual interpretation of the model evidences that leaf venations have the highest correlation in the plant recognition task.

1. Introduction

According to the FAO (Al et al., 2008), forests and trees contribute to growth economic, job creation, food security, energy generation and are fundamental to helping countries respond to climate change. The forestry industry produces more than 5000 timber products and generates a gross value added of more than US$ 600 billion annually, equivalent to 1% of the world's GDP. Whence, 80% of the forest resources are regulated by governments, which exploit their value chains and oversee its preservation and replacement programs following adequate forest management plans (Brito and Barreto, 2006; Soares-Filho et al., 2010).

1.1. Motivation

The Amazon forest represents the 21% of the global forest cover (Keenan et al., 2015) and has one of the richest diversities of tree species worldwide (O'neill et al., 2001; Wittmann et al., 2006). On the one hand, the Amazon Rainforest narrow global warming impact and provides natural resources to the many communities regardless of nationalities (Fearnside, 2008, 2012). On the other hand, timber resources are the main economic livelihood of the region (Barros and Uhl, 1999). However, despite authorities' efforts to regularize logging exploitation, the concessions usually commit violations to sustainability policies (Finer et al., 2014; Smith et al., 2006).

False figures declaration is one of the most common infringements, especially for valuable species like the Spanish cedar (*Cedrela odorata*) or the big-leaf mahogany (*Swietenia macrophylla*) (Finer et al., 2014).These deceits are a grave violation of the Convention on International Trade in Endangered Species of Wild Fauna and Flora (CITES). Whereby, species classification should be carried out by skilled botanists, but inside the deep Amazon, qualified experts are scarce and expensive (Ravindran et al., 2018). This situation worsens the control of not just endangered species but the full forest management plan.

In Peru, the Supervisory Agency for Forest and Wildlife Resources (OSINFOR) establishes the protocol on "Technical Criteria for the

* Corresponding author.
E-mail addresses: gerson.vizcarra@ucsp.edu.pe (G. Vizcarra), danitza.bermejo@gmail.com (D. Bermejo), manasses.mauricio@ucsp.edu.pe (A. Mauricio), rzarate@iiap.gob.pe (R. Zarate Gomez), edianderas@iiap.gob.pe (E. Dianderas).

https://doi.org/10.1016/j.ecoinf.2021.101268
Received 31 July 2020; Received in revised form 22 February 2021; Accepted 26 February 2021
Available online 18 March 2021
1574-9541/

Evaluation of Timber Resources". The protocol indicates that a "matero" (a non-technical person who recognizes the forest species at a common-name level) can support the identification to elaborate the forest management plan. If the task complicates, then a dendrology manual has to be used to verify the features of the tree. In case uncertainty persists, then an ex-situ analysis is necessary.

1.2. Proposed solution and contributions

As many authors mention (Azlah et al., 2019; Belhumeur et al., 2008; Jeon and Rhee, 2017; Keni and Ansari, 2017; Ni and Wang, 2018), machine learning algorithms can solve the plant species identification task using high-level leaves features. Regardless of the feature extraction technique, these tools require significant amounts of data that are unavailable for every case of study and even less in a specific context like deep Peruvian Amazon.

Deep Learning (DL) methods are at the top of the state-of-the-art on feature representation for different domains; albeit, DL lacks interpretability. According to Doshi-Velez and Kim (2017), interpretability lets human specialists understand what a model is learning, making them flexible real-world solutions. Given such topics, this paper has three significant contributions:

1. The paper introduces the first Peruvian Amazon Forestry Dataset, including its detailed metadata and the acquisition protocol description. The dataset collects 59,441 samples from ten of the most profitable and endangered species (Finer et al., 2014; Pinedo-Vasquez et al., 1992). Further-more, we employ six different commercial cameras to ensure variability and to develop any flexible solution with real-world conditions in the future.
2. A comparison of the four-top DL models for the leaf classification task: VGG-19 (Simonyan and Zisserman, 2014), AlexNet (Krizhevsky et al., 2012), DenseNet-201 (Huang et al., 2017), and ResNet-101 (He et al., 2016). Also, this work includes a visual interpretation algorithm to understand which specific leaf features the models learn.
3. A quantitative assessment of the background-removal relevance and model robustness for raw data. We make two training sets, one of the processed data and the other of raw data. Then, the models train with one dataset and test with the other one.

The upcoming sections are as follows: Section 2 contains the dataset description. Section 3 provides a literature review for the leaf classification task. Our contributions are explained in Section 4, while Section 5 shows the results. We discuss our findings in Section 6. Finally, Section 7 resumes our conclusions and future works.

2. Peruvian Amazon forestry dataset

Tree species classification is a complex task boarded from different approaches, including image processing. A specimen could be identified based on its flowers, barks, leaves, among others (Barbedo, 2016; Wäldchen and Mäder, 2018). A majority of studies use foliar features due to their high correlation in species identification. Furthermore, leaves preserve their physical characteristics almost all year, unlike flowers or fruits (Ellis, 2009). Consequently, we focus on leaves due to its morphological and texture information are well-enough to perform an accurate classification (Novotný and Suk, 2013; Thanh et al., 2018).

According to Wäldchen and Mäder (2018), there are three types of plant species identification datasets: scans, pseudo-scans, and photos. The first two correspond to images acquired through scanning and shooting samples with a simple background, respectively. Their configuration directly deals with occlusion, overlapping, and illumination problems. Photographic datasets correspond photographed specimens in the wild. Hitherto, the most reviewed large datasets of leaf images have come from North America (Belhumeur et al., 2008), North-eastern United States, and Canada (Kumar et al., 2012), China (Wu et al., 2007), and Europe (Novotný and Suk, 2013). These contributions, even though helpful, do not include Peruvian Amazon species, and do not share registration conditions.

The Peruvian Amazon Forestry Dataset[1] is a pseudo-scan collection of 59,441 leaf images of ten timber-tree species collected from the Allpahuayo-Mishana National Reserve, Peru. The species were selected because of their high commercialization, according to the OSINFOR's management information system.[2] Also, the species are included in the Peruvian official list of usable timber forest species (Resolution N 134–2016-SERFOR-DE). The images were gathered, labeled, and organized by researchers at the Instituto de Investigaciones de la Amazonía Peruana (IIAP) and high-skilled botanists. Metadata includes acquisition description (acquisition date, sensor type, spatial resolution, etc.) and taxonomy (scientific name, common name, taxonomic authority, taxonomic classification, synonyms, hierarchy, life form, life cycle, and reproduction).

2.1. Acquisition protocol

The samples are dark-background photos taken from six different commercial cameras, each one with different characteristics. We required five expeditions in different periods to build the dataset. Each journey follows the same acquisition protocol, which is (1) localization of specimens, (2) random recollection of leaves, and (3) massive digitization using a purple/black background. Initially, the purple background was defined to contrast better the leaf color due to its green predominance. However, the purple background could yield anomalous leaf color transformations according to the illumination. In consequence, we switched to a black background. This acquisition protocol ensures data variability and avoids over-fitting.

Fig. 1 presents a leaf from each specimen using their scientific names. Although all captures follow the same protocol, the ambient lighting varies according to the expedition date. Table 1 describes the cameras specifications which influence the registration (number of megapixels - Mpx, lens aperture, resolution and format). Fig. 2 shows the visual differences between the six camera models in similar lighting conditions for the species *Otoba glycycarpa* and *Cedrela odorata*.

2.2. Dataset distribution

Data distribution concerns the representativeness of classes since imbalances skew the models for specific features spaces. As a consequence, the predictions slope to the broader categories and model metrics increase. However, results in imbalance conditions are deceitful. As Table 2 shows, The Peruvian Amazon Forestry Dataset is almost balanced both by species and by devices.

2.3. Data variability

Two challenging qualities in an image classification dataset are the similarity among elements from different classes (inter-class correlation) and the diversity inside each class (intra-class coefficient). Like any real-world dataset, the Peruvian Amazon Forestry Dataset registers a high inter-class similarity and low intra-class correlation. Fig. 3a shows how similar four samples from different classes are (elliptic/ovate shapes), while Fig. 3b lays out the visual variation of four samples from the same specimen.

3. Related works

Over a decade ago, the feature engineering had established as

[1] http://teledeteccion.iiap.gob.pe/
[2] https://www.osinfor.gob.pe/sigo/

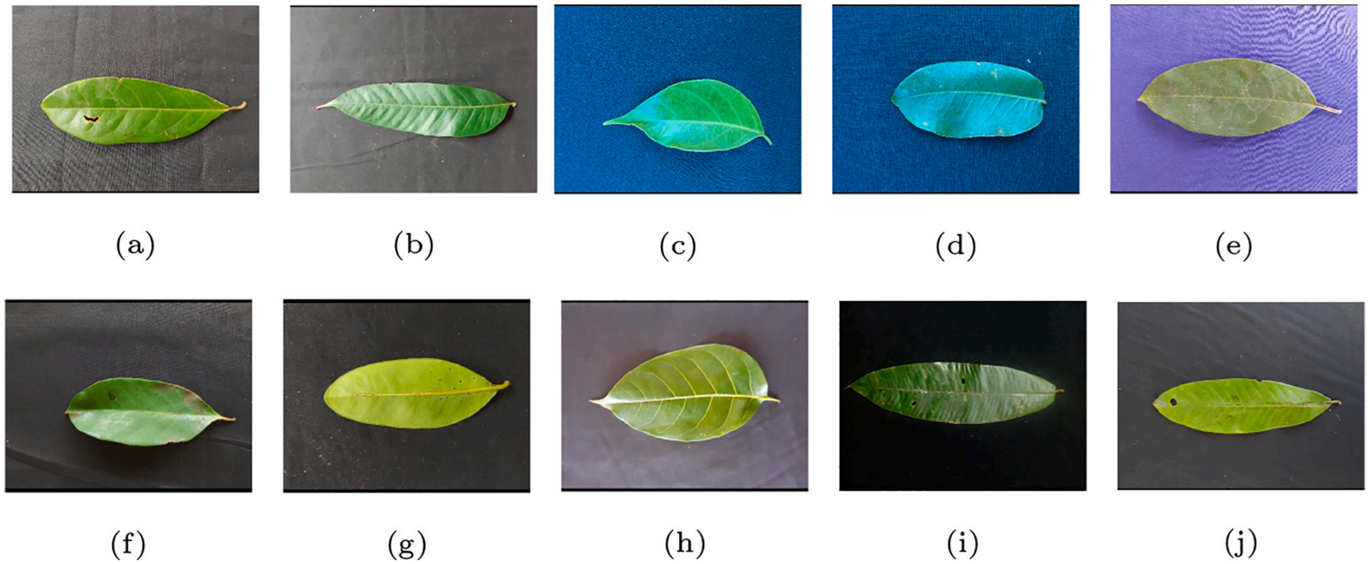

Fig. 1. Species from the Peruvian Amazon Forestry Dataset: (a) *Aniba rosaeodora*. (b) *Cedrela odorata*. (c) *Cedrelinga cateniformis*. (d) *Dipteryx micrantha*. (e)*Otoba glycycarpa*. (f) *Otoba parvifolia*. (g) *Simaruba amara*. (h) *Swietenia macrophworylla*. (i) *Virola flexuosa*. (j) *Virola pavonis*.

Table 1
Camera's specifications.

Code	Camera Model	Mpx	Aperture	Resolution	Format
DC	Nikon D3500	24.2	f/1.5	6000 × 4000	JPEG
CP1	SM-A705MN	32	f/1.7	4032 × 3024	JPEG
CP2	SM-A105M	13	f/1.9	4128 × 3096	JPEG
CP3	SM-A305G	16	f/2.0	4608 × 2128	JPEG
CP4	FIG-LX3	13	f/2.2	4160 × 3120	JPEG
CP5	IPhone6	8	f/2.2	3264 × 2448	JPEG

somewhat ambiguous methodology, but still useful, to define the best subset of features that represents a domain. Thenceforth, DL has risen to the very top of machine learning technologies, with promising results and tremendous potential in several applications, even agricultural (Kamilaris and Prenafeta-Boldú, 2018; Rawat and Wang, 2017; Zhang et al., 2020). This review focus on feature representation from hand-crafted and deep-learning perspectives.

3.1. Feature engineering

Feature engineering still has majority acceptance in the plant species identification task due to data limitations that cap the training step in DL models. Wäldchen and Mäder (2018) overhaul 120 research proposals considering the studied organ and features explored over different datasets. Leaf-features based recognition studies prevail by considering general features as shape (Belhumeur et al., 2008; Novotnỳ and Suk, 2013; Zhao et al., 2015), venation (Larese et al., 2014b,a), and texture (Olsen et al., 2015; Rashad et al., 2011). Features-reliability depends on dataset conditions and feature extraction technique (Thanikkal et al., 2017).

The majority of research papers focus on shape contour for classification. Belhumeur et al. (2008) match the shape of a query leaf with an ordered list of photographic collections by their Inner Distance Shape Context (IDSC). IDSC builds a 2D-histogram-descriptor at each sampled point along the boundary of leaves shape. Then, a non-Euclidean KNN algorithm ranks the most similar leaves by their histogram similarities. Novotnỳ and Suk (2013) include a 151 scanned species collection from Central Europe. After segmentation, Fourier descriptors normalize geometric features of the boundary. Different from previous studies, Zhao et al. (2015) introduce a counting-based shape descriptor, called Independent-IDSC, to classify global and local shape information independently.

Among leaf morphological characterizations, botanists mainly use

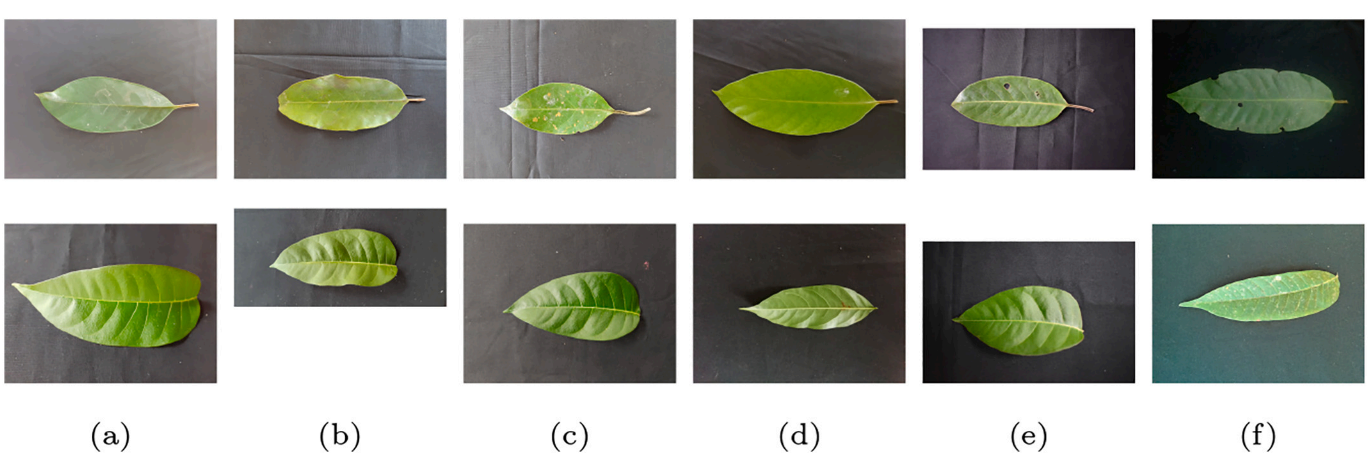

Fig. 2. Samples given different acquisition devices: (a) SM-A105M. (b) SM-A305G. (c) SM- A705MN. (d)FIG-LX3. (e) Nikon D3500. (f) iPhone 6. (Above) *Otoba glycycarpa*. (Below) *Cedrela odorata*.

Table 2
Data distribution over tree species (horizontal) and camera model (vertical).

Species	Samples						
	DC	CP1	CP2	CP3	CP4	CP5	Total
Aniba rosaeodora	1529	1547	1547	1537	402	–	6562
Cedrela odorata	1302	1302	1304	1303	188	127	5526
Cedrelinga cateniformis	1232	1232	1232	1230	177	176	5279
Dipteryx micrantha	1248	1248	1248	1248	480	340	5812
Otoba glycycarpa	1271	1281	1260	1268	136	322	5538
Otoba parvifolia	1745	1713	1712	1716	385	–	7271
Simaruba amara	980	1216	1216	1210	172	388	5182
Swietenia macrophylla	1564	1586	1568	1572	146	–	6436
Virola flexuosa	1030	1042	1040	1042	190	–	4344
Virola pavonis	1841	1842	1832	1840	136	–	7494
Total	13,742	14,009	13,959	13,966	2412	1353	**59,411**

Fig. 3. 3a Inter-class similarity: species *Otoba parvifolia*, *Otoba glycycarpa*, *Cedrela odorata*, *Swietenia macrophylla* (left to right). 3b Intra-class variation of *Aniba rosaeodora*.

the venation structures to recognize species (Park et al., 2008). The use of venations has its reason in the complexity and diversity among the shape contours of the leaves (Zhang et al., 2020). On the one hand, the leaves of different species could be similar in shape. On the other hand, the same specimen could have a high variance of leaf shapes. Larese et al. (2014b) classify three legume varieties based only on venations. First, they segment the venation by the unconstrained hit or miss transform (UHMT) and adaptive thresholding. LEAF-GUI-measures technique diversifies features from veins and areoles. Larese et al. (2014a) also explore a multiscale UHMT computation, concluding that the feature diversification improves results beyond classification technique.

On texture-based classification, Rashad et al. (2011) apply a Learning Vector Quantization (LVQ) alongside with a Radial Basis Function (RBF) in leaf image patches to outperform prior baselines. Olsen et al. (2015) propose a scale and rotation invariant enhancement of the Histogram of Oriented Gradients (HOG) to improve the representation of the texture. Their results suggest that the leaf skeleton stands out above other texture features.

3.2. Deep learning

The core of DL is the representation of multiple levels of abstraction by learning features from a dataset and extrapolating them to others. In the leaf image domain, Azlah et al. (2019) provide a review of techniques such as Bayesian, decision tree, k-nearest neighbor, support vector machine, probabilistic neural networks, and DL. In the same way, Zhang et al. (2020) present an overview of classic and DL methods to recognize plant species. Both works demonstrate that DL reaches better outcomes than traditional approaches to classify leaf images.

Despite its benefits, DL hauls fitting issues: under-fitting and over-fitting. On the one hand, under-fitting happens when the model is too simple to explain the variance. On the other hand, over-fitting implies that the model cannot be generalized to another dataset. Transfer learning (TL) is a well-known technique to overcome the fitting issues. The gist of TL is to fine-tune a model trained on one task or domain to another one related (Goodfellow et al., 2016).

Too et al. (2019) fine-tune CNN-based models (VGG, ResNet, Inception, and DenseNet) for plant species classification and disease detection. Qian et al. (2020) monitor invasive plant species in the wild by fine-tuned models (Alexnet, VGG, and GoogLeNet). Chulif et al. (2019) classify 10,000 plant species by using pre-trained InceptionNet models. Kaya et al. (2019) analyze deeply the effect of four different TL models on four publicly leaf datasets. (Barré et al., 2017) visualize that the first convolution layers learn to extract leaf venations and edges, while deeper layers derive high-level feature abstractions.

According to Lee et al. (2017), hierarchical orders in leaf venation are the most trustworthy high-level features. Grinblat et al. (2016) disentangle vein morphological patterns from color and leaf shape information. Next, a visualizing technique unveils relevant vein patterns. Other works explore joining morphological features such as vein and shape (Rizk, 2019; Thanh et al., 2018), or shape and texture (Shah et al., 2017).

4. Experiments

As seen in Fig. 1, raw images do not have lighting control or distance regulation between the leaf and the camera. However, noises are negligible, so there is no need to apply correction methods, except background removal due it adds texture noise in the boundary. Moreover, Image size depends on the camera model (Table 1), then images have to be resized and padded into the architecture requirements.

4.1. Background removal algorithm

Given the original image $\boldsymbol{I_{RGB}}$ composed by three matrices $\boldsymbol{I_R[i,j]}$, $\boldsymbol{I_G[i,j]}$ and $\boldsymbol{I_B[i,j]}$, being $\boldsymbol{i,j}$ the spatial coordinates in the image. A sharpening filter enhances the $\boldsymbol{I_{RGB}}$'s edges definition using a Gaussian Blur operation ($\boldsymbol{\Psi}$). Eq. (1) denotes the morphological process per pixel per channel for $\boldsymbol{I_{RGB}}$, where $\boldsymbol{I^s_{RGB}}$ is the output.

$$\begin{aligned} I^s_R[i,j] &= 1.5\cdot I_R[i,j] - 0.5\cdot\Psi(I_R[i,j]) \\ I^s_G[i,j] &= 1.5\cdot I_G[i,j] - 0.5\cdot\Psi(I_G[i,j]) \\ I^s_B[i,j] &= 1.5\cdot I_B[i,j] - 0.5\cdot\Psi(I_B[i,j]) \end{aligned} \tag{1}$$

Next, we turn $\boldsymbol{I^s_{RGB}}$ to Lab color space to boost colors and definitions. Lab color space approximates human vision rather than describing how colors should appear on digital (RGB) or in print (CMYK). According to Fan and Wang (2013), the translation from RGB to Lab color space is a two-step process. We must translate RGB space to XYZ space (Eq. (2)), then translate it into Lab space (Eq. (4)) using the $\boldsymbol{f}$-function (Eq. (3)).

$$\begin{aligned} I^s_X[i,j] &= 0.4124\cdot I^s_R[i,j] + 0.3576\cdot I^s_G[i,j] + 0.1805\cdot I^s_B[i,j] \\ I^s_Y[i,j] &= 0.2126\cdot I^s_R[i,j] + 0.7152\cdot I^s_G[i,j] + 0.0722\cdot I^s_B[i,j] \\ I^s_Z[i,j] &= 0.0193\cdot I^s_R[i,j] + 0.1192\cdot I^s_G[i,j] + 0.9505\cdot I^s_B[i,j] \end{aligned} \tag{2}$$

$$f(t) = \begin{cases} \sqrt[3]{t}, & \textit{if } t > 0.0089 \\ 7.7871\cdot t + 0.1379, & \textit{otherwise} \end{cases} \tag{3}$$

$$\begin{aligned} I^s_L[i,j] &= 116\cdot f\left(\frac{I^s_Y[i,j]}{100}\right) - 16 \\ I^s_a[i,j] &= 500\cdot\left(f\left(\frac{I^s_X[i,j]}{95.0489}\right) - f\left(\frac{I^s_Y[i,j]}{100}\right)\right) \\ I^s_b[i,j] &= 200\cdot\left(f\left(\frac{I^s_Y[i,j]}{100}\right) f\left(\frac{I^s_Z[i,j]}{108.8840}\right)\right) \end{aligned} \tag{4}$$

We highlight $\boldsymbol{I^s_{Lab}}$ by using the contrast limited adaptive histogram equalization (Pizer et al., 1987) on the $\boldsymbol{L}$ (lightness) channel getting $\boldsymbol{I^h_{Lab}}$. When returning to the RGB color space ($\boldsymbol{I^h_{RGB}}$) (Eqs. (5), (6) and (7)), the leaf color at each pixel has a predominance of green over blue.

$$f^{-1}(t) = \begin{cases} t^3, & \textit{if } t > 0.2069 \\ 0.1284\cdot t + 0.0177, & \textit{otherwise} \end{cases} \tag{5}$$

$$\begin{aligned} I^h_X[i,j] &= 95.0489\cdot f^{-1}\left(\frac{I^h_L[i,j]+16}{116} + \frac{I^h_a[i,j]}{500}\right) \\ I^h_Y[i,j] &= 100\cdot f^{-1}\left(\frac{I^h_L[i,j]+16}{116}\right) \\ I^h_Z[i,j] &= 108.8840\cdot f^{-1}\left(\frac{I^h_L[i,j]+16}{116} - \frac{I^h_b[i,j]}{200}\right) \end{aligned} \tag{6}$$

$$\begin{aligned} I^h_R[i,j] &= 3.2405\cdot I^h_X[i,j] - 1.5371\cdot I^h_Y[i,j] - 0.4985\cdot I^s_Z[i,j] \\ I^h_G[i,j] &= -0.9693\cdot I^s_X[i,j] + 1.8760\cdot I^h_Y[i,j] + 0.0416\cdot I^s_Z[i,j] \\ I^h_B[i,j] &= 0.0556\cdot I^s_X[i,j] - 0.2040\cdot I^h_Y[i,j] + 1.0572\cdot I^s_Z[i,j] \end{aligned} \tag{7}$$

Henceforth, a mask performs a partial background removal following the Eq. (8).

$$Mask[i,j] = \begin{cases} 1, & \textit{if } I^h_G[i,j] > \left(I^h_B[i,j] + 20\right) \\ 0, & \textit{otherwise} \end{cases} \tag{8}$$

We only mask the green channel ($\boldsymbol{I^h_G}$) due it brings out edges (Eq. (9)). A bilateral filter $\boldsymbol{BF}$ (Tomasi and Manduchi, 1998) is then applied to mitigate small noises and preserve relevant boundaries resulting in $\boldsymbol{I^b_G}$.

$$\boldsymbol{I^b_G[i,j] = BF\left(I^h_G[i,j]\cdot Mask[i,j]\right)} \tag{9}$$

Similar to Fang et al. (2009), the Otsu's algorithm in $\boldsymbol{I^b_G}$ computes the Otsu's optimal threshold value ($\boldsymbol{\Omega}$), which we employ to calculate the two thresholds ($\boldsymbol{\theta_{Low}}$ and $\boldsymbol{\theta_{High}}$) in the Canny edge detector (Canny, 1986). Eq. (10) shows the computation of both thresholds by manual tuning. The double-threshold step in the Canny edge detector identifies 3 kinds of pixels (strong, weak, and non-relevant) depending on its relationship with final edges (Eq. (11)). Finally, the algorithm chooses the most massive object and fills it via a morphological closing operation (erosion ⊖ and dilation ⊕ using a circle-shaped structuring element $\boldsymbol{SE}$ of diameter 15) to get the final segmentation mask $\boldsymbol{Mask^F}$ (Eq. (12)).

$$\begin{aligned} \boldsymbol{\theta_{Low}} &= \boldsymbol{\frac{\Omega - 29.75}{1.41}} \\ \boldsymbol{\theta_{High}} &= \boldsymbol{\theta_{Low}\cdot 6} \end{aligned} \tag{10}$$

$$\boldsymbol{I_{Canny} = Canny\left(I^b_G, \theta_{Low}, \theta_{High}\right)} \tag{11}$$

$$\boldsymbol{Mask^F = \left(I_{Canny} \oplus SE\right) \ominus SE} \tag{12}$$

The final segmentation mask is applied to the original image in order to remove the background of it getting $\boldsymbol{I^f_{RGB}}$ (Eq. (13)). Fig. 4 displays stage-by-stage the background removal procedure.

$$\begin{aligned} \boldsymbol{I^f_R[i,j]} &= \boldsymbol{Mask^F[i,j]\cdot I_R[i,j] I^f_G[i,j] = Mask^F[i,j]\cdot I_G[i,j] I^f_B[i,j]} \\ &= \boldsymbol{Mask^F[i,j]\cdot I_B[i,j]} \end{aligned} \tag{13}$$

4.2. Architecture configurations

Convolutional neural networks (CNN) outstand over DL techniques by disentangling high-level representations across multiple processing layers. CNN's process data on two levels: a convolutional block for the automatic feature extraction, and fully connected layers to establish feature-output correlation. The convolutional block comprises convolutional, ReLU, and max-pooling layers. Each set of convolutional layers diversify features by applying a set of parallel filters that process local sections of the input space. The feature vector integrates low-level local features from the first layers and higher-level representations from the latest ones.

Like any other complex model, DL requires a large amount of data to fit appropriately, which is hard in our context. To overcome this limitation, we employ different architectures pre-trained with the ImageNet dataset. Pre-trained models capture low-level features (e.g., edges, corners, color spots, etc.) from one domain and transfer them to another with similar characteristics. The transfer process is called fine-tuning due to the model only learns specific higher-level features (e.g., arrangements, venations, etc.). We compare four pre-trained models: (1) AlexNet (Krizhevsky et al., 2012, 2) VGG-19 (Simonyan and Zisserman, 2014, 3) ResNet-101 (He et al., 2016, 4) DenseNet-201 (Huang et al., 2017). The fully connected block is adjusted to feed off the feature vector and output the ten species of leaves. Table 3 describe architecture characteristics

4.3. Training details

We split the dataset by the camera model: DC, CP1, and CP2 models are for training/validation, and CP3, CP4, and CP5 for testing. The

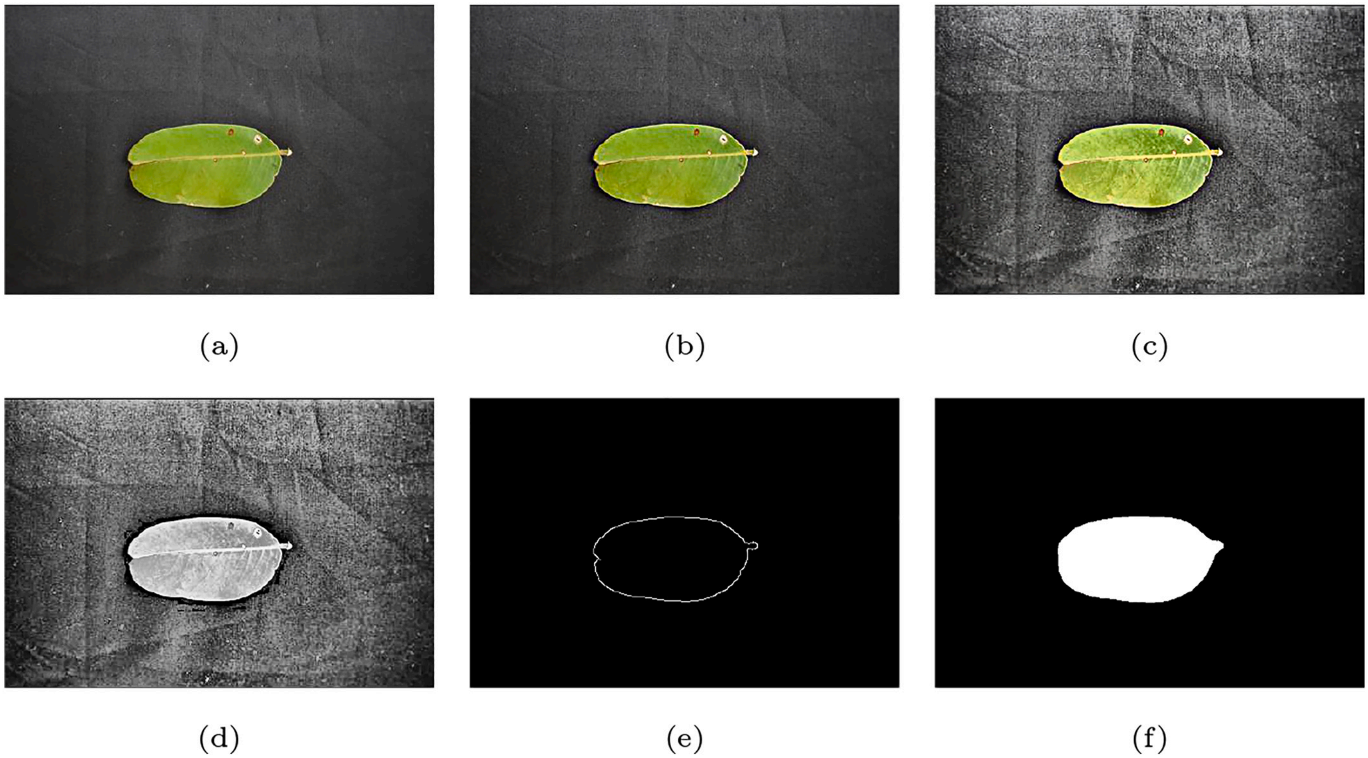

Fig. 4. Intermediate results of the background removal algorithm: (4a) Input image - I_{RGB} (4b) Sharpen Image I^S_{RGB}. (4c) Adaptive equalization of the Lightness - I^H_{RGB}. (4d) Masked green channel - I^H_G. (4e) Canny edge detection applied on $I^b_G - I_{Canny}$. (4f) Final. (For interpretation of the references to color in this figure legend, the reader is referred to the web version of this article.)
segmentation mask - $Mask^{F.}$

Table 3
Architectures comparison: AlexNet, VGG-19, ResNet-101, and DenseNet-201.

Network	Year	Depth	#parameters
AlexNet	2012	8	60 M
VGG-19	2014	19	144 M
ResNet-101	2016	101	44.8 M
DenseNet-201	2017	201	20 M

validation samples are selected randomly from the first group. The data distribution is 70.12% for training, 1.69% validation, and 28.19% for testing. The model feeds off with 16 elements per mini-batches using the ADAM optimizer (Kingma and Ba, 2014) with a learning rate of 1e-3. To run our experiments, we use Pytorch 1.3 framework in a PC with the following specifications: 4.0 GHz Intel Core i9 processor, 32 GB 3000 MHz DDR4 memory, and NVIDIA Titan RTX.

5. Results

Considering that DL lacks intrinsic interpretability, we introduce a visual-interpretability module that supports our qualitative analysis and expand the quantitative results. The quantitative results allow us to weight the impact of each stage (pre-processing and fine-tuning) in terms of accuracy. At the same time, visual interpretation lets us understand what the model is looking at in the input space.

5.1. Quantitative evaluation

The pre-processing stage reduces noises and standardizes inputs, which enhances metrics. Nevertheless, real-world data challenges robustness for any model due to registration conditions are not in control. Therefore, we run an experimental ablation in the background removal algorithm to measure if the model learns by itself how to focus on the leaf beyond background.

Table 4 shows the accuracy of the fine-tuned models using pre-processed images and raw ones. First, we observe that pre-processed images do not enhance any model's result. Second, AlexNet and VGG-19 models provide better outcomes comparing to ResNet-101 and DenseNet-201 (around 10%). Therefore, the models with more layers perform more complex transformations than those required for our dataset.

Ideally, a robust model must classify accurately, regardless of background or input noises. We analyze the model's behavior by swapping testing sets between pre-processed and raw images (Table 5). The experimental results on model robustness show that the models suffer an accuracy drop. This drop varies depending on the training data: >13% for raw images, and > 17% for pre-trained ones. Furthermore, ResNet-101 and DenseNet-201 decrease up to 52%. These figures draw that AlexNet and VGG-19 are ideal for our context.

To make an in-depth analysis of the CNNs performance, we evaluate the champion model (VGG-19) when predicting each specie. Fig. 5 show the confusion matrices of two trained VGG-19 on raw (Fig. 5a) and pre-processed (Fig. 5b) testing sets, respectively. The confusion matrices show that the model generalize well in all species, albeit it is not symetric. This condition is not odd in multi-class tasks; however, data imbalances increase asymmetry. The most peculiar case occurs between Cedrelinga cateniformis and Swietenia macrophylla classes in raw conditions. The first one has greater confusion ratio respect to the second one than in reverse. In contrast, Fig. 5b shows that pre-processed images relieve this phenomenon.

5.2. Qualitative evaluation

Like Lee et al. (2017) and Barré et al. (2017), the qualitative evaluation consists of a visual interpretation of features. Instead of visualizing features per layer, we apply the Integrated Gradients (Sundararajan

Table 4
Accuracy of the models w/wo pre-processing.

Model	Accuracy					
	Raw			Pre-processed		
	Train	Validation	Test	Train	Validation	Test
AlexNet	**98.75%**	97.16%	**96.16%**	**98.21%**	**97.92%**	95.98%
VGG-19	96.77%	**98.30%**	95.15%	96.94%	**97.92%**	**96.52%**
ResNet-101	82.25%	89.04%	83.30%	77.25%	79.02%	75.44%
DenseNet-201	93.71%	91.30%	86.48%	91.61%	87.33%	86.29%

Table 5
Accuracy of the models swapping the testing sets (source → target).

Model	Accuracy	
	Raw → Pre-processed	Pre-processed → Raw
AlexNet	82.35%	54.76%
VGG-19	**82.70%**	**78.87%**
ResNet-101	69.22%	29.56%
DenseNet-201	65.26%	33.97%

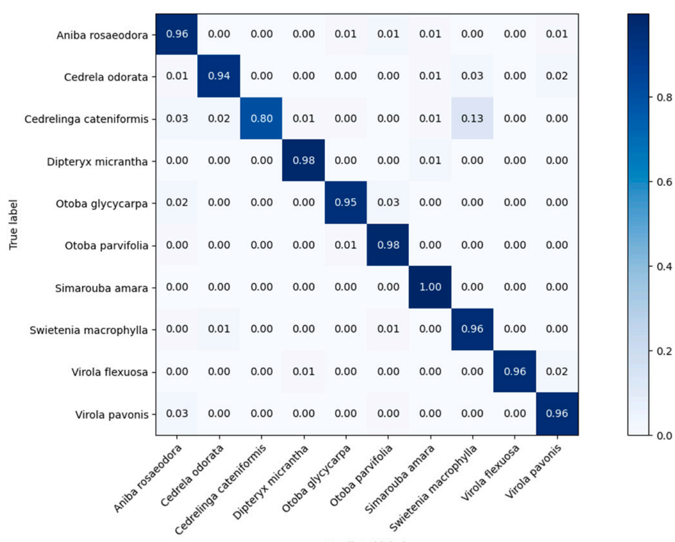

(a) Confusion matrix of the VGG-19 architecture for the raw testing set.

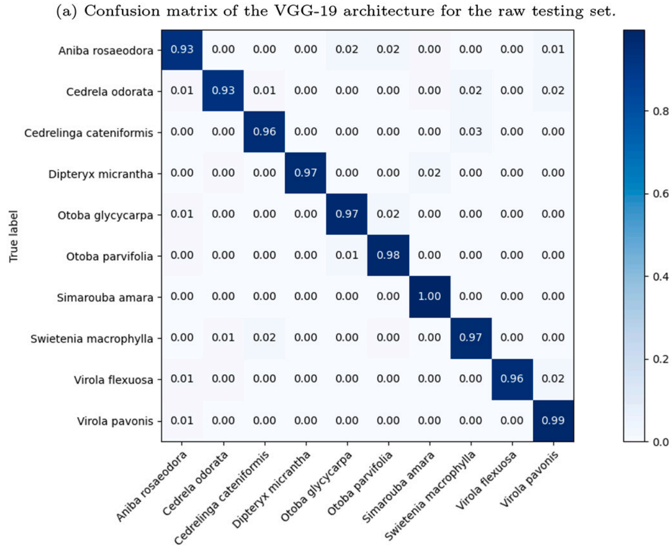

(b) Confusion matrix of the VGG-19 architecture for the pre-processed testing set.

Fig. 5. Confusion matrices for the VGG-19 architecture.

et al., 2017) and SmoothGrad (Smilkov et al., 2017) methods over each model. These methods plot a point cloud, where the density denotes the input space relevance. Thus, a higher density in a region suggests that the network ponderates it the most when classifying.

Figs. 6 and 7 show the visual representation of features when fine-tuning with raw and segmented images, respectively. These results bolster the ones gets in qualitative analysis (Table 4). AlexNet and VGG-19 learn high-level leaf features, such as venations and shapes (VGG-19 more than AlexNet). Moreover, the models fine-tuned with the raw dataset fit even better than the other ones. A clear example of this observation is the ResNet-101 fine-tuned with pre-processed images (Fig. 7). This model has learned to classify based on lateral sections, almost ignoring the leaf. So, the fine-tuned ResNet-101 probably have exploited an error in the background removal algorithm of some images.

6. Discussion

Traditionally, ResNet-101, and DenseNet-201 have been considered inside the top-models for general feature extraction task, especially the ones related with ImageNet Kornblith et al. (2019). Nevertheless, our quantitative and qualitative evaluations evidence that AlexNet and VGG-19 are superior for The Peruvian Amazon Forestry Dataset since both derive high-quality abstractions.

AlexNet achieves to extract shape, texture, and venation with some noise, while VGG-19 focus strongly in shape and venation. Consequently, VGG-19 has remarkable results in different leaf image processing tasks (Lee et al., 2017; Rizk, 2019; Thanh et al., 2018).

Skip connections mitigate singularities related to the deactivation of units, breaking the linear dependence of the network (Orhan and Pitkow, 2018). Residual connections are useful to explore different levels of features maps in complex datasets since mid to high-level abstractions. However, our qualitative evaluation suggests that skip connections could add noise in scan/pseudo scan leaf classification.

Background removal algorithms are a standard in pre-processing pipelines to ensure that models focus on leaves instead of background (Belhumeur et al., 2008; Cruz et al., 2019; da Silva et al., 2019; Novotný and Suk, 2013; Zhao et al., 2015). However, this step does not yield significant improvements, it even worsens accuracy in some settings when models exploit segmentation errors. Conversely, by using raw images, the model learns to ignore the background itself and becomes more robust. Those statements agree with prior works (Goeau et al., 2017; Krause et al., 2016).

7. Conclusions and future works

In this paper, we present the Peruvian Amazon Forestry Dataset, including leaf images of ten species. It is important to remark that a public database is a contribution by itself since it allows the development of new research works in the area focused on the Peruvian Amazon conditions. Our aim is to move forward the control of endangered timber species by providing a resource to classify them automatically. Instead of delving into the creation of feature representation, such as in previous approaches, we reverse engineer the process by asking DL to interpret and elicit the particular features that best represent the leaf data. Based on the results, we strongly suggest using the models AlexNet and VGG-

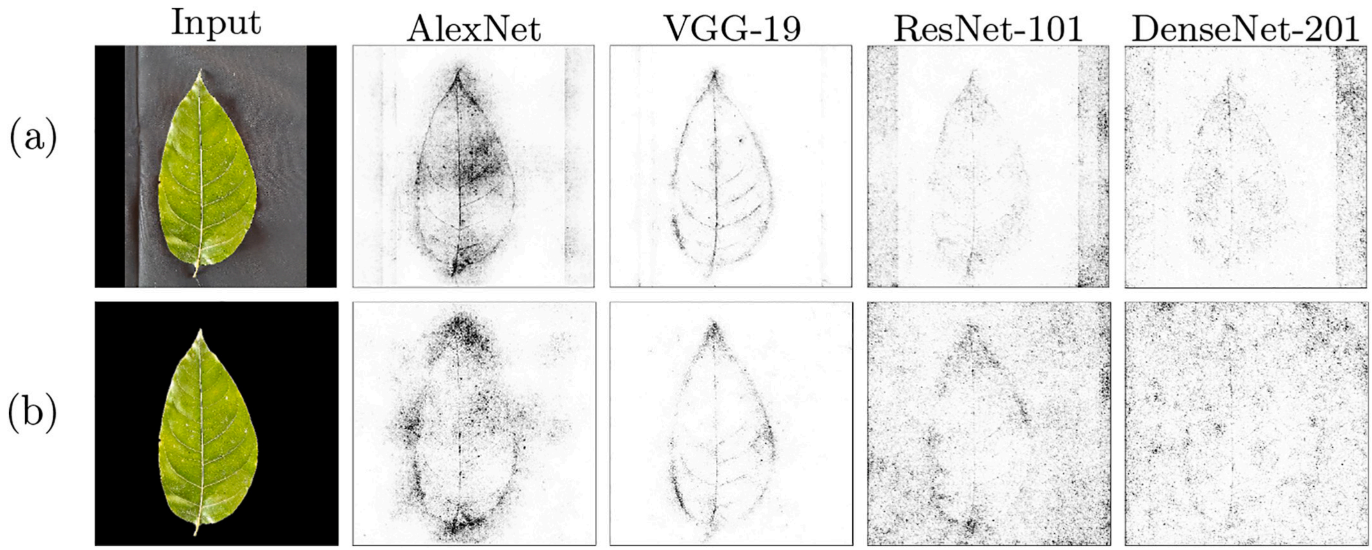

Fig. 6. Feature visualization of the models (trained with raw images) given a (a) raw input, or a (b) pre-processed input.

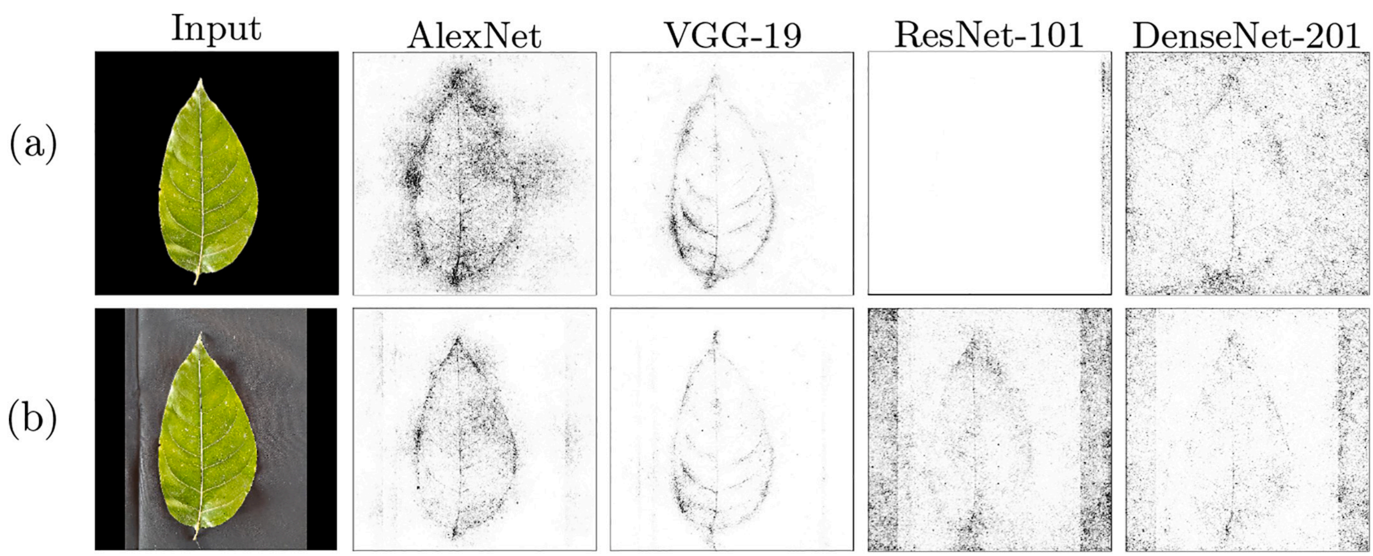

Fig. 7. Feature visualization of the models (trained with raw images) given a (a) raw input, or a (b) pre-processed input.

19 for future real-world solutions. The interpretation results suggest that venations and shape are the most trustworthy morphological features. That reflects the trivial knowledge researchers intuitively deploy in their imaginative vision from the outset. Finally, this study demonstrates the benefits of training models with raw inputs to achieve robustness and accuracy. In future studies, we will explore end-to-end solutions and extending the dataset by adding more species.

Funding

The present work was carried out under the grant 022-2018- FONDECYT-BM-IADT-AV, thanks to the "Fondo Nacional de Desarrollo Científico, Tecnológico y de Innovación Tecnológica (FONDECYT)", Peru, an initiative of the "Consejo Nacional de Ciencia, Tecnología e Innovación Tecnologíca (CONCYTEC)", Peru.

Declaration of Competing Interest

The authors declare that they have no known competing financial interests or personal relationships that could have appeared to influence the work reported in this paper.

Acknowledgements

Authors would like to thank Linder Mozombite-Pinto and Milagros Rimachi Taricuarima for their collaboration during the collection phase of this research.

References

Al, W., Orking, G., Clima, O., 2008. Climate Change and Food Security: a Framework Document. FAO Rome.

Azlah, M.A.F., Chua, L.S., Rahmad, F.R., Abdullah, F.I., Wan Alwi, S.R., 2019. Review on techniques for plant leaf classification and recognition. Computers 8, 77. https://doi.org/10.3390/computers8040077.

Barbedo, J.G.A., 2016. A review on the main challenges in automatic plant disease identification based on visible range images. Biosyst. Eng. 144, 52–60. https://doi.org/10.1016/j.biosystemseng.2016.01.017.

Barré, P., Stöver, B., Müller, K., Steinhage, V., 2017. Leafnet: a computer vision system for automatic plant species identification. Ecol. Info. 40, 50–56. https://doi.org/10.1016/j.ecoinf.2017.05.005.

Barros, A.C., Uhl, C., 1999. The economic and social significance of logging operations on the floodplains of the amazon estuary and prospects for ecological sustainability. Adv. Econ. Bot. 13, 153–168.
Belhumeur, P.N., Chen, D., Feiner, S., Jacobs, D.W., Kress, W.J., Ling, H., Lopez, I., Ramamoorthi, R., Sheorey, S., White, S., et al., 2008. Searching the world's herbaria: a system for visual identification of plant species. In: European Conference on Computer Vision. Springer, pp. 116–129. https://doi.org/10.1007/978-3-540-88693-8_9.
Brito, B., Barreto, P., 2006. Enforcement against illegal logging in the brazilian amazon. In: 4th IUCN Academy of Environmental Law Colloquium. IUCN.
Canny, J., 1986. A computational approach to edge detection. In: IEEE Transactions on Pattern Analysis and Machine Intelligence, pp. 679–698.
Chulif, S., Jing Heng, K., Wei Chan, T., Al Monnaf, M., Chang, Y.L., 2019. Plant identification on amazonian and guiana shield flora: Neuon submission to lifeclef 2019 plant. In: CLEF (Working Notes).
Cruz, A., Ampatzidis, Y., Pierro, R., Materazzi, A., Panattoni, A., De Bellis, L., Luvisi, A., 2019. Detection of grapevine yellows symptoms in vitis vinifera l. with artificial intelligence. Comput. Electron. Agric. 157, 63–76. https://doi.org/10.1016/j.compag.2018.12.028.
da Silva, L.A., Bressan, P.O., Gonçalves, D.N., Freitas, D.M., Machado, B.B., Gonçalves, W.N., 2019. Estimating soybean leaf defoliation using convolutional neural networks and synthetic images. Comput. Electron. Agric. 156, 360–368. https://doi.org/10.1016/j.compag.2018.11.040.
Doshi-Velez, F., Kim, B., 2017. Towards a rigorous science of interpretable machine learning. arXiv. URL. https://arxiv.org/abs/1702.08608.
Ellis, B., 2009. Manual of Leaf Architecture. Published in association with the New York Botanical Garden.
Fan, H., Wang, W., 2013. Edge detection of color road image based on lab model. In: 2013 International Conference on Computational and Information Sciences. IEEE, pp. 298–301.
Fang, M., Yue, G., Yu, Q., 2009. The study on an application of otsu method in canny operator. In: Proceedings. The 2009 International Symposium on Information Processing (ISIP 2009). Citeseer, p. 109.
Fearnside, P.M., 2008. Amazon forest maintenance as a source of environmental services. An. Acad. Bras. Cienc. 80, 101–114. https://doi.org/10.1590/S0001-37652008000100006.
Fearnside, P.M., 2012. Brazil's amazon forest in mitigating global warming: unresolved controversies. Clim. Pol. 12, 70–81. https://doi.org/10.1080/14693062.2011.581571.
Finer, M., Jenkins, C.N., Sky, M.A.B., Pine, J., 2014. Logging concessions enable illegal logging crisis in the peruvian amazon. Sci. Rep. 4, 4719. https://doi.org/10.1038/srep04719.
Goeau, H., Bonnet, P., Joly, A., 2017. Plant identification based on noisy web data: the amazing performance of deep learning (lifeclef 2017). In: CLEF: Conference and Labs of the Evaluation Forum 1866. Dublin, Ireland. URL. https://hal.archives-ouvertes.fr/hal-01629183.
Goodfellow, I., Bengio, Y., Courville, A., 2016. Deep Learning. MIT press.
Grinblat, G.L., Uzal, L.C., Larese, M.G., Granitto, P.M., 2016. Deep learning for plant identification using vein morphological patterns. Comput. Electron. Agric. 127, 418–424. https://doi.org/10.1016/j.compag.2016.07.003.
He, K., Zhang, X., Ren, S., Sun, J., 2016. Deep residual learning for image recognition. In: Proceedings of the IEEE Conference on Computer Vision and Pattern Recognition, pp. 770–778. https://doi.org/10.1109/CVPR.2016.90.
Huang, G., Liu, Z., Van Der Maaten, L., Weinberger, K.Q., 2017. Densely connected convolutional networks. In: 2017 IEEE Conference on Computer Vision and Pattern Recognition (CVPR), pp. 2261–2269. https://doi.org/10.1109/CVPR.2017.243.
Jeon, W.-S., Rhee, S.-Y., 2017. Plant leaf recognition using a convolution neural network. Int. J. Fuzzy Logic Intell. Syst. 17, 26–34. https://doi.org/10.5391/IJFIS.2017.17.1.26.
Kamilaris, A., Prenafeta-Boldú, F.X., 2018. Deep learning in agriculture: a survey. Comput. Electron. Agric. 147, 70–90. https://doi.org/10.1016/j.compag.2018.02.016.
Kaya, A., Keceli, A.S., Catal, C., Yalic, H.Y., Temucin, H., Tekinerdogan, B., 2019. Analysis of transfer learning for deep neural network based plant classification models. Comput. Electron. Agric. 158, 20–29. https://doi.org/10.1016/j.compag.2019.01.041.
Keenan, R.J., Reams, G.A., Achard, F., de Freitas, J.V., Grainger, A., Lindquist, E., 2015. Dynamics of global forest area: results from the fao global forest resources assessment 2015. For. Ecol. Manag. 352, 9–20. https://doi.org/10.1016/j.foreco.2015.06.014.
Keni, N.D., Ansari, R.A., 2017. Content based image retrieval for leaf identification using structural features and neural networks. In: 2017 4th International Conference on Signal Processing and Integrated Networks (SPIN). IEEE, pp. 298–303. https://doi.org/10.1109/SPIN.2017.8049963.
Kingma, D.P., Ba, J., 2014. Adam: A Method for Stochastic Optimization. arXiv preprint arXiv:1412.6980.
Kornblith, S., Shlens, J., Le, Q.V., 2019. Do better imagenet models transfer better?. In: Proceedings of the IEEE Conference on Computer Vision and Pattern Recognition, pp. 2661–2671. https://doi.org/10.1109/CVPR.2019.00277.
Krause, J., Sapp, B., Howard, A., Zhou, H., Toshev, A., Duerig, T., Philbin, J., Fei-Fei, L., 2016. The unreasonable effectiveness of noisy data for fine-grained recognition. In: European Conference on Computer Vision. Springer, pp. 301–320. https://doi.org/10.1007/978-3-319-46487-9_19.
Krizhevsky, A., Sutskever, I., Hinton, G.E., 2012. Imagenet classification with deep convolutional neural networks. In: Advances in Neural Information Processing Systems, pp. 1097–1105.
Kumar, N., Belhumeur, P.N., Biswas, A., Jacobs, D.W., Kress, W.J., Lopez, I.C., Soares, J.V., 2012. Leafsnap: a computer vision system for automatic plant species identification. In: European Conference on Computer Vision. Springer, pp. 502–516. https://doi.org/10.1007/978-3-642-33709-3_36.
Larese, M.G., Bayá, A.E., Craviotto, R.M., Arango, M.R., Gallo, C., Granitto, P.M., 2014a. Multiscale recognition of legume varieties based on leaf venation images. Expert Syst. Appl. 41, 4638–4647. https://doi.org/10.1016/j.eswa.2014.01.029.
Larese, M.G., Namías, R., Craviotto, R.M., Arango, M.R., Gallo, C., Granitto, P.M., 2014b. Automatic classification of legumes using leaf vein image features. Pattern Recogn. 47, 158–168. https://doi.org/10.1016/j.patcog.2013.06.012.
Lee, S.H., Chan, C.S., Mayo, S.J., Remagnino, P., 2017. How deep learning extracts and learns leaf features for plant classification. Pattern Recogn. 71, 1–13. https://doi.org/10.1016/j.patcog.2017.05.015.
Ni, F., Wang, B., 2018. Integral contour angle: an invariant shape descriptor for classification and retrieval of leaf images. In: 2018 25th IEEE International Conference on Image Processing (ICIP). IEEE, pp. 1223–1227. https://doi.org/10.1109/ICIP.2018.8451605.
Novotný, P., Suk, T., 2013. Leaf recognition of woody species in central europe. Biosyst. Eng. 115, 444–452. https://doi.org/10.1016/j.biosystemseng.2013.04.007.
Olsen, A., Han, S., Calvert, B., Ridd, P., Kenny, O., 2015. In situ leaf classification using histograms of oriented gradients. In: 2015 International Conference on Digital Image Computing: Techniques and Applications (DICTA). IEEE, pp. 1–8. https://doi.org/10.1109/DICTA.2015.7371274.
O'neill, G.A., Dawson, I., Sotelo-Montes, C., Guarino, L., Guariguata, M., Current, D., Weber, J.C., 2001. Strategies for genetic conservation of trees in the peruvian amazon. Biodivers. Conserv. 10, 837–850. https://doi.org/10.1023/A:1016644706237.
Orhan, E., Pitkow, X., 2018. Skip connections eliminate singularities. In: International Conference on Learning Representations. URL. https://openreview.net/forum?id=HkwBEMWCZ.
Park, J., Hwang, E., Nam, Y., 2008. Utilizing venation features for efficient leaf image retrieval. J. Syst. Softw. 81, 71–82. https://doi.org/10.1016/j.jss.2007.05.001.
Pinedo-Vasquez, M., Zarin, D., Jipp, P., 1992. Economic returns from forest conversion in the peruvian amazon. Ecol. Econ. 6, 163–173.
Pizer, S.M., Amburn, E.P., Austin, J.D., Cromartie, R., Geselowitz, A., Greer, T., ter Haar Romeny, B., Zimmerman, J.B., Zuiderveld, K., 1987. Adaptive histogram equalization and its variations. Comp. Vision Graphics Image Proc. 39, 355–368. https://doi.org/10.1016/S0734-189X(87)80186-X.
Qian, W., Huang, Y., Liu, Q., Fan, W., Sun, Z., Dong, H., Wan, F., Qiao, X., 2020. Uav and a deep convolutional neural network for monitoring invasive alien plants in the wild. Comput. Electron. Agric. 174, 105519. https://doi.org/10.1109/CVPR.2015.7298594.
Rashad, M., El-Desouky, B., Khawasik, M.S., 2011. Plants images classification based on textural features using combined classifier. Int. J. Comp. Sci. Info. Technol. 3, 93–100. https://doi.org/10.5121/ijcsit.2011.3407.
Ravindran, P., Costa, A., Soares, R., Wiedenhoeft, A.C., 2018. Classification of cites-listed and other neotropical meliaceae wood images using convolutional neural networks. Plant Methods 14, 25. https://doi.org/10.1186/s13007-018-0292-9.
Rawat, W., Wang, Z., 2017. Deep convolutional neural networks for image classification: a comprehensive review. Neural Comput. 29, 2352–2449. https://doi.org/10.1162/neco_a_00990.
Rizk, S., 2019. Plant Leaf Classification using Dual Path Convolutional Neural Networks. Ph.D. thesis. Notre Dame University-Louaize.
Shah, M.P., Singha, S., Awate, S.P., 2017. Leaf classification using marginalized shape context and shape+ texture dual-path deep convolutional neural network. In: 2017 IEEE International Conference on Image Processing (ICIP). IEEE, pp. 860–864. https://doi.org/10.1109/ICIP.2017.8296403.
Simonyan, K., Zisserman, A., 2014. Very deep convolutional networks for large-scale image recognition. arXiv preprint arXiv:1409.1556.
Smilkov, D., Thorat, N., Kim, B., Viégas, F., Wattenberg, M., 2017. Smoothgrad: removing noise by adding noise. arXiv preprint arXiv:1706.03825.
Smith, J., Colan, V., Sabogal, C., Snook, L., 2006. Why policy reforms fail to improve logging practices: the role of governance and norms in Peru. Forest Policy Econ. 8, 458–469. https://doi.org/10.1016/j.forpol.2005.08.001.
Soares-Filho, B., Moutinho, P., Nepstad, D., Anderson, A., Rodrigues, H., Garcia, R., Dietzsch, L., Merry, F., Bowman, M., Hissa, L., et al., 2010. Role of brazilian amazon protected areas in climate change mitigation. In: Proceedings of the National Academy of Sciences, 107, pp. 10821–10826. https://doi.org/10.1073/pnas.0913048107.
Sundararajan, M., Taly, A., Yan, Q., 2017. Axiomatic attribution for deep networks. In: Proceedings of the 34th International Conference on Machine Learning, Vol. 70, pp. 3319–3328.
Thanh, T.K.N., Truong, Q.B., Truong, Q.D., Xuan, H.H., 2018. Depth learning with convolutional neural network for leaves classifier based on shape of leaf vein. In: Asian Conference on Intelligent Information and Database Systems. Springer, pp. 565–575. https://doi.org/10.1007/978-3-319-75417-8_53.
Thanikkal, J.G., Dubey, A.K., Thomas, M., 2017. Whether color, shape and texture of leaves are the key features for image processing based plant recognition? An analysis!. In: 2017 Recent Developments in Control, Automation & Power Engineering (RDCAPE). IEEE, pp. 404–409. https://doi.org/10.1109/RDCAPE.2017.8358305.
Tomasi, C., Manduchi, R., 1998. Bilateral filtering for gray and color images. In: Sixth International Conference on Computer Vision (IEEE Cat. No. 98CH36271). IEEE, pp. 839–846.

Too, E.C., Yujian, L., Njuki, S., Yingchun, L., 2019. A comparative study of fine-tuning deep learning models for plant disease identification. Comput. Electron. Agric. 161, 272–279. https://doi.org/10.1016/j.compag.2018.03.032.

Wäldchen, J., Mäder, P., 2018. Plant species identification using computer vision techniques: a systematic literature review. Arch. Comp. Methods Eng. 25, 507–543. https://doi.org/10.1007/s11831-016-9206-z.

Wittmann, F., Schöngart, J., Montero, J.C., Motzer, T., Junk, W.J., Piedade, M.T., Queiroz, H.L., Worbes, M., 2006. Tree species composition and diversity gradients in white-water forests across the amazon basin. J. Biogeogr. 33, 1334–1347. https://doi.org/10.1111/j.1365-2699.2006.01495.x.

Wu, S.G., Bao, F.S., Xu, E.Y., Wang, Y.-X., Chang, Y.-F., Xiang, Q.-L., 2007. A leaf recognition algorithm for plant classification using probabilistic neural network. In: 2007 IEEE International Symposium on Signal Processing and Information Technology. IEEE, pp. 11–16. https://doi.org/10.1109/ISSPIT.2007.4458016.

Zhang, S., Huang, W., Huang, Y.-A., Zhang, C., 2020. Plant species recognition methods using leaf image: overview. Neurocomputing. https://doi.org/10.1016/j.neucom.2019.09.113.

Zhao, C., Chan, S.S., Cham, W.-K., Chu, L., 2015. Plant identification using leaf shapes - a pattern counting approach. Pattern Recogn. 48, 3203–3215. https://doi.org/10.1016/j.patcog.2015.04.004.